ENHANCING PV MODULE THERMOMECHANICAL PERFORMANCE AND RELIABILITY BY AN INNOVATIVE MOUNTING SOLUTION

Andreas J. Beinert[1], Alex Masolin[2]
[1]Fraunhofer Institute for Solar Energy Systems ISE, Heidenhofstraße 2, 79110 Freiburg, Germany
[2]Coolback Company B.V., Amstelveenseweg 500, 1081 KL Amsterdam, The Netherlands
Corresponding author: Andreas J. Beinert | Phone: +49 (0)761 4588 5630 | E-mail: Andreas.Beinert@ise.fraunhofer.de

ABSTRACT: Using mechanical finite element method simulations, we compare the mechanical stability of an innovative mounting solution for PV modules to that of a conventionally framed module. The innovative mounting solution (Coolback® system) is a combined mounting and passive cooling structure which replaces the backsheet and the frame. We simulate the mechanical load test comparing a conventionally framed module to one using the Coolback® system. Both laminates are identical and consist of a 60-cell and a 144-half-cell/72-cell configuration. The finite element method simulations show that the cooling fins reduce the deflection of the module significantly, resulting in negligible solar cell fracture probabilities for all loads. Especially at high loads, where the framed module has a high solar cell fracture probability, the increased mechanical stability caused by the cooling fins helps to reduce cell fracturing.

Keywords: Finite element modelling, FEM simulations, module mounting, module frame, mechanical load, photovoltaic module, stress, thermomechanics, virtual prototyping.

1 INTRODUCTION

With the increasing number of PV installations in hot regions with high solar radiation, the demand is growing for methods to decrease the operating temperature in PV modules, therefore increasing the energy output. One attempt is to place cooling structures on the rear side of the PV module. In this work, we investigate such an approach called Coolback® from a thermomechanical point of view with the finite element method (FEM). The Coolback® system utilizes cooling fins to replace a conventional frame and backsheet (Figure 1). Integration takes place during the solar module manufacturing process. Additionally, the system has specific clamps to swiftly mount a module on rails without tools (click system) which have been considered in the FEM analysis.

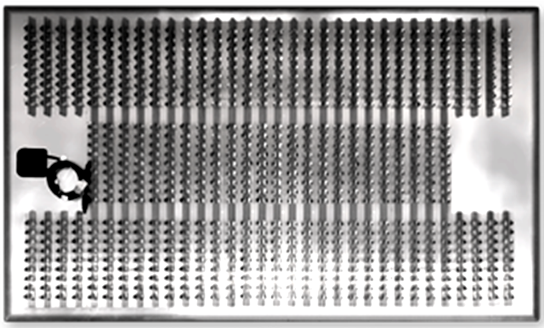

Figure 1: Coolback® cooling fins on the rear side of a PV module.

We investigate the mechanical performance of a 60-cell PV module using such cooling fins by performing FEM simulations of mechanical push and pull load according to IEC 61215 [1]. The result is compared with the FEM simulation of a conventionally framed module using an identical laminate, considering the maximum deflection and the probability of solar cell fracture. Currently, the market is trending towards larger module sizes. Therefore, a PV module with 144-half-cells and cooling fins is simulated and compared to a framed module with 72-full-cells. For both mounting structures, the lamination process is simulated prior to attaching the mounting structure. The aim is to assess the impact of a structural element that covers the entire rear side of the module in comparison to the conventional edge frame mounting solution in mechanical load.

2 METHOD

The FEM model used is based on a FEM model published previously [2,3]. The solar cells are implemented as full-square mono-crystalline silicon wafers, without metallization and ribbons. We use hexahedral mesh elements with 2,700 mesh elements per full solar cell and a quadratic serendipity basis function. Exploiting the two-fold axial symmetry, we model a quarter laminate.

The FEM model covers lamination and mechanical load (ML) in push and pull direction. For ML, either a conventional frame or the Coolback® cooling fins are attached to the conventional laminate structure (glass-encapsulant-backsheet). We simulate the mounting of the framed module on a rack by a fixed constraint on the long side of the module with a distance of 22% of the long side to its edge. Details of the frame were published previously [4]. As for the cooling fins, the PV module is mounted by specially designed clamps from the bottom, as shown in Figure 2. For the 60-full-cell module, four clamps are used. To account for the larger module area, 10 clamps are used for the 144-half-cell module.

We simulate the lamination process by applying cooling from 150 °C to 25 °C. The residual stress from lamination is considered in the ML simulation. We simulate a homogeneous push load of 2400 Pa and 5400 Pa as well as a pull load of 2400 Pa. The used material models are shown in Table I.

To assess the impact of the novel mounting system, we evaluate the FEM simulation results using the maximum deflection of the PV module and the principal stresses in the solar cells. As a brittle material, silicon solar cells fail under tensile stress, therefore, we evaluate the maximum of the first principal stress σ_I within the solar cells. We convert the obtained maximum first

Table I: Specifications and material properties of the PV module with frame and with Coolback® profiles (cooling fins). *: provided by the manufacturer, †: measured. Please note, that the solar cell dimension belongs to a full cell, a half cell has the same width, but a length of 78.375 mm.

Layer	Material	Dimension	Density [g/cm³]	Young's modulus [GPa]	Poisson's ratio [-]	CTE [$10^{-6}K^{-1}$]
Front glass	soda-lime glass	3.2 mm	2.5*	70*	0.2*	9*
Encapsulant	EVA	460 µm	0.96 [11]	T-dep.†	0.4 [11]	270 [11]
Solar Cell	Cz silicon	156.75 × 156.75 × 0.180 mm³	2.329 [11]	Elasticity matrix [11]		T-dep. [9,10]
Backsheet	TPT	295 µm	2.52 [11]	3.5 [11]	0.29 [11]	50.4 [11]
Frame	aluminum		2.7 [12]	70 [12]	0.33 [12]	23 [12]
Frame-inlay	rubber	8.85 × 1.15 mm²	0.067*	0.0074*	0.3*	769*
Coolback ® profile	aluminum		2.7*	69.5*	0.33*	T-dep.*
Adhesive		50 µm	1.05*	0.87*	0.3*	270*

principal stress σ_I values from the front and back side of the solar cells into a probability of solar cell fracture P_f using the Weibull distribution [5] considering the size effect [6]:

$$P_\mathrm{f} = 1 - \exp\left(-\sum_\mathrm{i} A_\mathrm{eff,i} \left(\frac{\sigma_\mathrm{I,max}}{\sigma_\mathrm{0,i}} \right)^{m_\mathrm{i}} \right), \qquad (1)$$

with the effective area A_eff, the maximum first principal stress $\sigma_\mathrm{I,max}$, the Weibull scale factor σ_0 and the Weibull modulus m. The sum is calculated over the values of the front (sunny) and back side, respectively. The effective area A_eff can be interpreted as the area of significant stress values and is calculated for the front and back side separately by:

$$A_\mathrm{eff,i} = \int \left(\frac{\sigma_\mathrm{I,i}(\mathrm{x,y})}{\sigma_\mathrm{I,max}} \right)^{m_\mathrm{i}} dA_\mathrm{i}\,. \qquad (2)$$

The probability of solar cell fracture P_f expresses the likelihood that, within one module, at least one crack in at least one solar cell occurs. For the Weibull scale factor σ_0 and modulus m we use values from Kaule *et al.* [7] for Al-BSF solar cells. Mono- and bifacial PERC solar cells have a very similar behavior [8]. However, there are significant differences to other solar cell architectures. Therefore, the presented cell fracture probabilities are just exemplary and the evaluation has to be performed for a specific cell type individually.

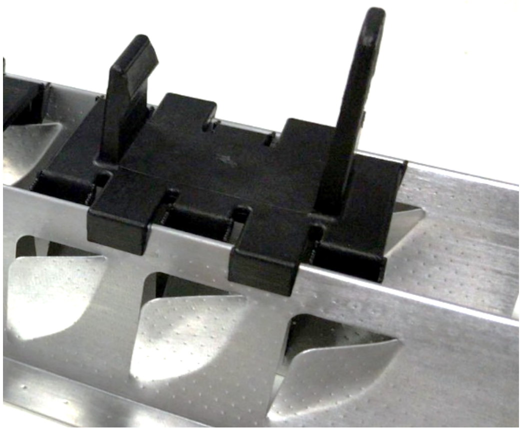

Figure 2: Detailed view of one cooling fin with the specially designed clamps.

3 RESULTS

Figure 4 shows the deflection d of all configurations at 2400 Pa push load. The maximum deflection d for all loads is depicted in Figure 3.

Firstly, we discuss the 60-cell configurations. For all investigated load cases, the PV module with cooling fins has a significantly lower maximum deflection. The cooling fins also lead to a different deflection shape. Instead of the parabolic deflection of a conventionally framed PV module, the PV module with cooling fins shows a rather U-shaped deflection and, thus a smaller curvature (Figure 4).

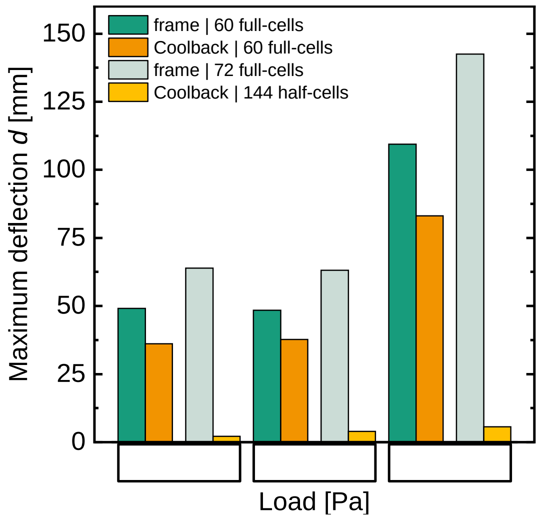

Figure 3: Maximum deflection of the different configurations for all simulated loads. Note: in the Coolback® configuration, four clamps are used for 60-cells and ten clamps are used for 144-half-cells.

Figure 5 depicts the maximum first principal stress σ_I along with the corresponding probability of solar cell fracture P_f. At 2400 Pa pull load, the PV module with cooling fins has a higher maximum first principal stress of 42 MPa than the framed PV module with 7 MPa. This originates from the mounting on the rear side by the clamps, around which very local tensile stress is induced due to the bending. However, since this is only small area, the solar cell fracture probability is still negligible. At 2400 Pa push load, the PV module with cooling fins

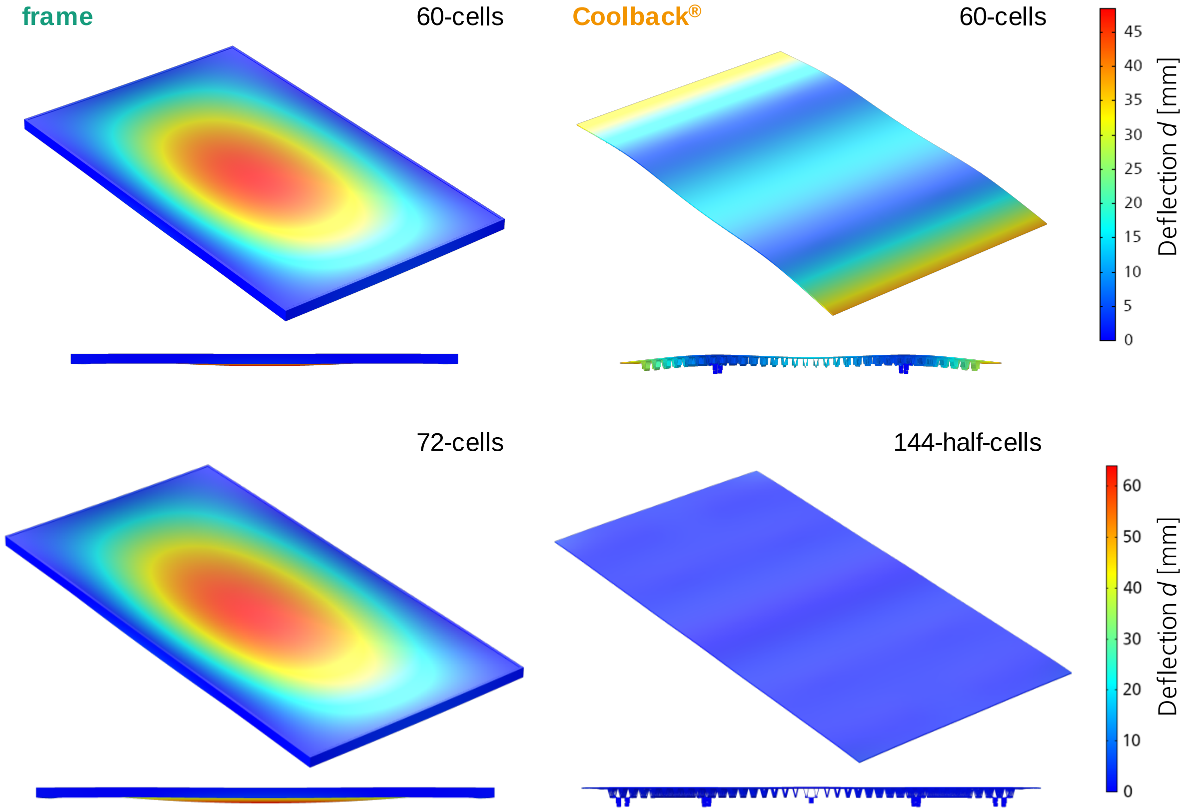

Figure 4: Simulated deflection at 2400 Pa push load in isometric and side view. Left: Conventional frame, right: Coolback® cooling fins, top: 60 cells, bottom: 72 cells / 144 half-cells. Please note, that in the Coolback® configuration for 60 cells four clamps and for 144 half-cells ten clamps are used.

shows a lower tensile stress of 8 MPa compared to 24 MPa in the framed PV module. Both values correspond to negligible solar cell fracture probabilities. When going to 5400 Pa push load, the difference in tensile stress increases for the PV module with cooling fins reaching 30 MPa and the framed PV module reaching 128 MPa. This corresponds to a solar cell fracture probability of 48% for the framed PV module, while the module with cooling fins still shows a negligible value. Therefore, the cooling fins reduce the risk of cell fractures, especially for high loads.

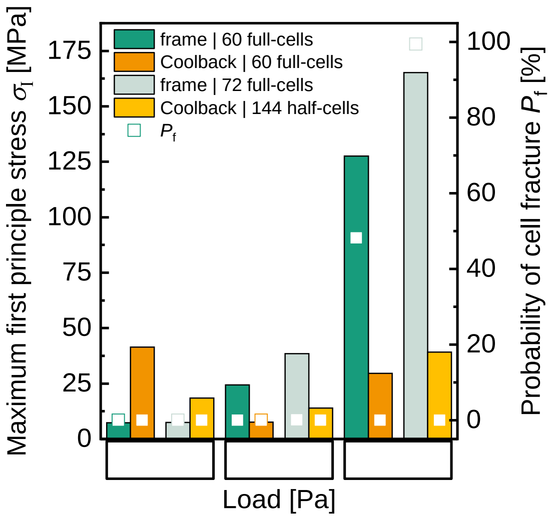

Figure 5: Maximum first principal stress σ_I (left axis) with the corresponding probability of cell fracture P_f (right axis) for all configurations and loads. Note: in the Coolback® configuration, four clamps are used for 60 cells and ten clamps are used for 144 half-cells.

Secondly, we discuss the configuration with 72-full-cells and 144-half-cells, respectively, using a 10-clamp set-up. In this configuration, the deflection is further reduced to almost negligible values (4 mm at 2400 Pa push load). This shows the effectiveness of increasing the number of clamps from four (60 cells) to ten (144 half-cells). The framed 72-cell module has a significantly higher maximum deflection for all loads (63 mm at 2400 Pa push load). Therefore the 144 half-cells module with cooling fins has a lower maximal stress and corresponding solar cell fracture probability P_f. At push loads, tensile stress is induced due to the local stress around the clamps. However, the higher number of clamps reduces the induced stress from 36 MPa (60-cells) to 19 MPa (144-half-cells).

The opposite is the case for push loads. Here, the 60-cell configuration has slightly lower tensile stress values than the 144-half-cell configuration because there is a cell edge directly above one of the clamps. For this reason, the cell exhibits a relatively high curvature, which induces tensile stress. This can easily be reduced by changing the clamp positions. However, stress is not critical for all loads and corresponds to negligible solar cell fracture probabilities. Comparing this to the 99% solar cell fracture probability of the framed module at 5400 Pa, shows that the rear side mounting solution provided by the cooling fins increases the mechanical stability of PV modules significantly. This reduces the risk and the amount of cell cracks, especially for large PV modules.

4 CONCLUSIONS

We use FEM simulations to compare a structural element that covers the entire rear side of the module with a conventional frame. We find that cooling fins in combination with rear side mounting reduce the tensile stress within the solar cells at push load. Our simulations show, that especially at high push loads, the different deflection shape leads to fewer solar cells exposed to high tensile stress and, accordingly, to negligible solar cell fracture probabilities. For a 60-cell module at 5400 Pa push load, the solar cell fracture probability is negligible for the configuration with cooling fins, while for the framed module it is 48%. The solar cell fracture probability increases to 99% for the larger framed module with 72-cells, while the probability remains negligible for the module with 144-half-cells and cooling fins. Therefore, a module utilizing a rear side mounting with cooling fins is likely more robust against push loads. Exposed to pull loads, the maximum deflection is lower for the module with cooling fins. Due to local tensile stress around the clamp, however, the maximum tensile stress is lower for the laminate with a conventional frame, in both sizes. Nevertheless, all configurations have negligible solar cell fracture probabilities at 2400 Pa pull load. Therefore, the cooling fins in combination with a rear side mounting may increase the mechanical stability of a module significantly and reduce the risk of cell cracks.

6 REFERENCES

[1] IEC IEC 61215-2:2016, Terrestrial photovoltaic (PV) modules – Design qualification and type approval – Part 2: Test procedures (2016).

[2] A.J. Beinert, P. Romer, M. Heinrich, M. Mittag, J. Aktaa, H. Neuhaus, Proceedings of the 36th European Photovoltaic Solar Energy Conference and Exhibition (EU PVSEC) (2019), 783–788.

[3] A.J. Beinert, P. Romer, M. Heinrich, M. Mittag, J. Aktaa, H. Neuhaus, IEEE J. Photovolt. 10 (2020), 70–77.

[4] A.J. Beinert, M. Ebert, U. Eitner, J. Aktaa, Proceedings of the 32nd European Photovoltaic Solar Energy Conference and Exhibition (EU PVSEC) (2016), 1833–1836.

[5] W. Weibull A Statistical Theory of the Strength of Materials, Generalstabens Litografiska Anstalts Förlag, Stockholm (1939).

[6] D. Munz, T. Fett Ceramics: Mechanical properties, failure behaviour, materials selection, 1st ed., Springer, Berlin | Heidelberg (2001).

[7] F. Kaule, M. Pander, M. Turek, M. Grimm, E. Hofmueller, S. Schönfelder, AIP Conference Proceedings 1999 (2018), pp. 020013-1–020013-9.

[8] F. Kaule, S. Meyer, S. Schönfelder, Proceedings of the 33rd European Photovoltaic Solar Energy Conference and Exhibition (EU PVSEC) (2017), 276–279.

[9] R.B. Roberts, Journal of Physics D: Applied Physics 14 (1981), L163-163.

[10] R.B. Roberts, Journal of Physics D: Applied Physics 15 (1982), L119-120.

[11] U. Eitner, S. Kajari-Schroeder, M. Köntges, H. Altenbach, in: H. Altenbach, V.A. Eremeyev (Eds.), Shell-like Structures: Non-classical Theories and Applications, Springer, Berlin/Heidelberg, 2011.

[12] W.M. Haynes (Ed.) CRC handbook of chemistry and physics, CRC Press, 2014.